

# The global distribution of depositional rivers on early Mars

J.L. Dickson<sup>1\*</sup>, M.P. Lamb<sup>1</sup>, R.M.E. Williams<sup>2</sup>, A.T. Hayden<sup>1</sup> and W.W. Fischer<sup>1</sup>

<sup>1</sup>Division of Geological and Planetary Sciences, California Institute of Technology (Caltech), 1200 E. California Boulevard, Pasadena, California 91125, USA

<sup>2</sup>Planetary Science Institute, 1700 East Fort Lowell, Suite 106, Tucson, Arizona 85719, USA

## ABSTRACT

**Sedimentary basins are the archives of ancient environmental conditions on planetary surfaces, and on Mars they may contain the best record of surface water and habitable conditions. While erosional valley networks have been mapped, the global distribution of fluvial sedimentary deposits on Mars has been unknown. Here we generated an eight-trillion-pixel global map of Mars using data from the NASA Context Camera (CTX), aboard the Mars Reconnaissance Orbiter spacecraft, to perform the first systematic global survey of fluvial ridges—exhumed ancient deposits that have the planform shape of river channels or channel belts, but stand in positive relief due to preferential erosion of neighboring terrain. We used large fluvial ridges (>70 m width) as a conservative proxy for the occurrence of depositional rivers or river-influenced depositional areas. Results showed that fluvial ridges are as much as 100 km long, common across the southern highlands, occur primarily in networks within intercrater plains, and are not confined to impact basins. Ridges were dominantly found in Noachian through Late Hesperian units, consistent with cessation of valley network activity, and occurred downstream from valley networks, indicating regional source-to-sink transport systems. These depositional areas mark a globally distributed class of sedimentary deposits that contain a rich archive of Mars history, including fluvial activity on early Mars.**

## INTRODUCTION

A major goal in Mars science is to understand the surface environments billions of years ago when Mars had active rivers on its surface (Carr, 1996). Sedimentary rocks are primary archives of environmental history, and on Earth, their study has led to our understanding of the evolution of the atmosphere, oceans, continents, and biosphere (Miall, 2010). Thick strata accumulated in subsiding basins on Earth, sourced in part via net depositional river systems (Allen, 1997). It is unclear whether this large-scale source-to-sink model is appropriate for Mars (Grotzinger et al., 2013). In particular, the global catalog of fluvial erosion on early Mars (Hynek et al., 2010) is better documented than the record of fluvial sedimentary deposits. Deposits within craters have been mapped systematically at the local scale (Cabrol and Grin, 1999; Fassett and Head, 2008b; Goudge et al., 2015) and non-systematically at the global scale due to lack of global imaging (Howard et al.,

2005; Moore and Howard, 2005; Irwin et al., 2005). There has yet to be a systematic survey of fluvial ridges—exhumed ancient fluvial deposits (Burr et al., 2009; Williams et al., 2009, 2011, 2013; DiBiase et al., 2013; Davis et al., 2016, 2019; Cardenas et al., 2018; Hayden et al., 2019; Balme et al., 2020)—across the entire surface of Mars, which may potentially hold a yet richer record of environmental conditions than the topographic record of eroded valley networks.

Unlike the surface of Earth, which is continually modified, Mars has had minimal tectonic activity and experienced cold and hyperarid conditions since valley network cessation (Fassett and Head, 2008a), which has led to the preservation of erosional landforms in regions that have not been resurfaced. Fluvial deposits on Mars may also be relatively well preserved compared to Earth, but their deposits are accessible only where they have been partially exhumed. Here we used the occurrence of fluvial ridges as a conservative proxy for river-influenced net depositional areas, in contrast to valley networks that are net erosional river valleys. Fluvial ridges are

landforms that have the appearance of sinuous or branching fluvial channels, or river channel belts, in planform but stand as topographic highs (Figs. 1 and 2) (Williams et al., 2009). Many of these features are fluvial deposits exhumed due to preferential erosion of weaker surrounding strata (e.g., floodplain mudstone) (Burr et al., 2009). Some ridges may be exhumed channel fills, while others likely represent larger channel-belt deposits that typify the internal architecture of fluvial strata (Burr et al., 2009, 2010; Williams et al., 2011; Cardenas et al., 2018; Hayden et al., 2019).

## METHODS

Our goal was not to replicate the detailed investigations that have been done using targeted high-resolution data of ridges; e.g., in Arabia Terra (Hynek and Phillips, 2001; Davis et al., 2016, 2019) and the Medusae Fossae Formation (Burr et al., 2009; Cardenas et al., 2018; Hayden et al., 2019). Instead, we systematically mapped the global distribution of ridges to understand where fluvial-influenced depositional areas occur outside of craters, and whether they are associated with valley networks as source-to-sink systems. Systematic surveys that use global coverage (1) eliminate targeting bias (Williams, 2007), and (2) provide confidence regarding interpretations as to where features of interest occur and, equally importantly, where they do not occur.

We mapped ridges by eye across the entire planet using the first global mosaic of data from the NASA Context Camera (CTX) aboard the Mars Reconnaissance Orbiter (MRO) spacecraft (Malin et al., 2007), rendered at 5.0 m/px (Dickson et al., 2018). We mapped ridges as polyline features by direct observation, without regard to previous identifications to avoid inherited bias. We used a compilation of ridge locations independently mapped (Williams, 2007) to assess our identification uncertainty (Table S1 in the Supplemental Material<sup>1</sup>). We mapped all fluvial

\*E-mail: [jdickson@caltech.edu](mailto:jdickson@caltech.edu)

<sup>1</sup>Supplemental Material. Table of all fluvial ridge systems mapped in this study. Please visit <https://doi.org/10.1130/GEOL.S.13312943> to access the supplemental material, and contact [editing@geosociety.org](mailto:editing@geosociety.org) with any questions.

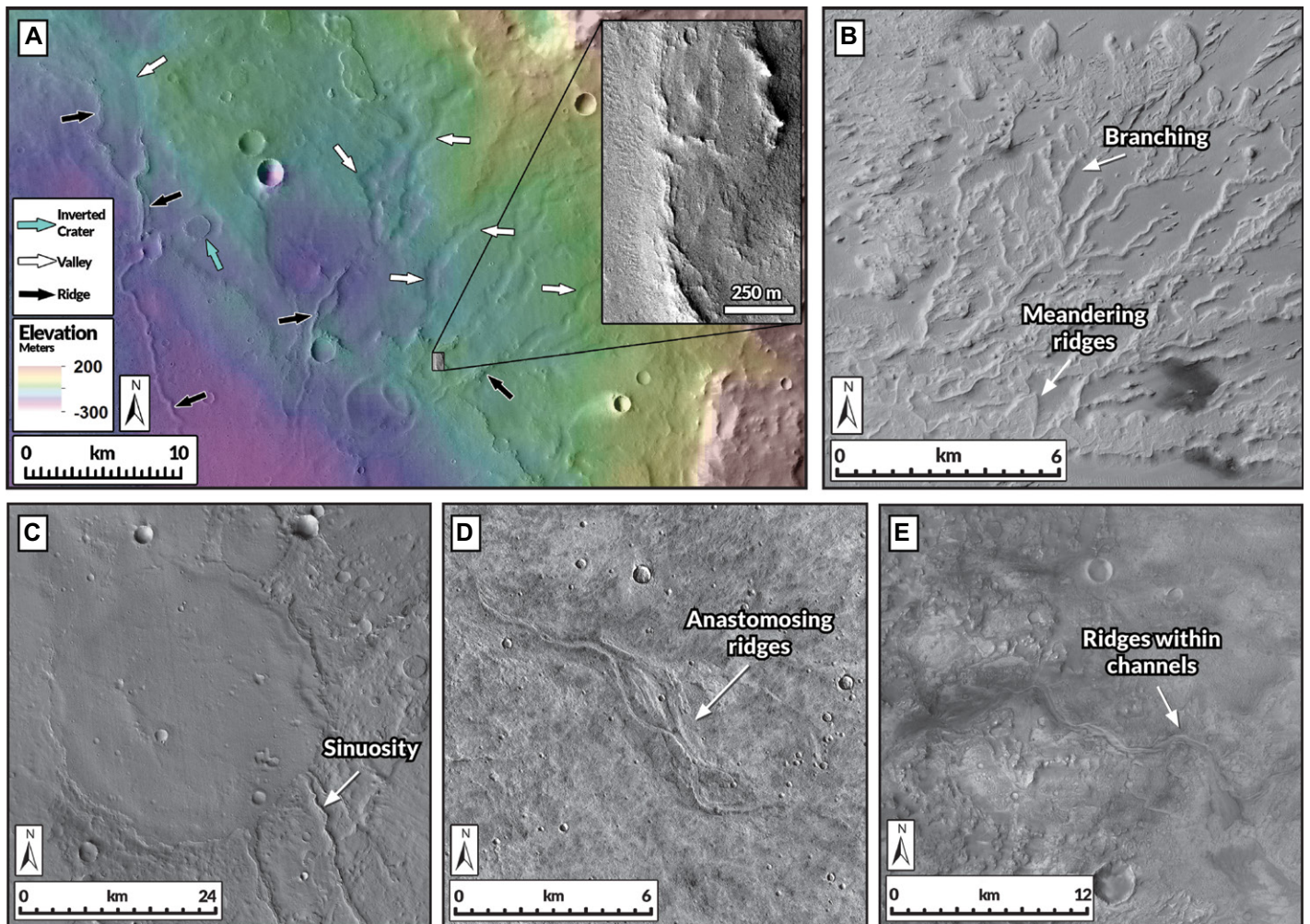


**Figure 1.** Fluvial ridge morphology on Mars and relationships with adjacent units. (A) NASA Context Camera (CTX) mosaic of Arabia Terra with Mars Orbiter Laser Altimeter (MOLA) topography of fluvial ridges (black arrows) emanating downslope from valley networks and eroding out of a broader sedimentary unit (Davis et al., 2016). 7.6°N, 26.3°E. Inset: High Resolution Imaging Science Experiment (HiRISE) orbit ESP\_058721\_1875. (B) Flat-topped fluvial ridges within Aeolis Dorsum in CTX data. These ridges show branching and meandering patterns. In our mapping, systems of ridges are represented by a single marker in Figure 3. (C) CTX mosaic of fluvial ridges in direct contact with exhumed crater fills in Arabia Terra. 16.1°N, 50.0°E. (D) Anastomosing ridges observed in CTX data in cratered plains west of Alba Patera. 43.7°N, 232.4°E. (E) Fluvial ridge in CTX data confined within an existing valley upstream of the western fan within Jezero crater. 18.8°N, 76.9°E.

ridges globally with widths  $> \sim 70$  m. While we did observe smaller ridges, they were found on alluvial (Kraal et al., 2008) and deltaic (Fassett and Head, 2008b) fans—these reflect local depositional environments, most commonly within crater basins, and have been the focus of previous studies (Fassett and Head, 2008b; Kraal et al., 2008; Goudge et al., 2015).

Fluvial ridges were identified following criteria laid out in previous work (Burr et al., 2009; Williams et al., 2011; Davis et al., 2016, 2019; Cardenas et al., 2018; Hayden et al., 2019). Ridges that met at least two of the following criteria were included in our survey: (1) presence of sinuosity over the scale of kilometers (Fig. 1), (2) consistent topographic trends along regional topography (as measured with data from the Mars Orbiter Laser Altimeter aboard the Mars Global Surveyor spacecraft) for ridges within a network (Fig. 1A), (3) branching patterns

(Fig. 1D), (4) consistent crest morphology, and (5) occurrence in proximity to a valley network system (Figs. 1A and 1E). Ridges with lobate flows emanating symmetrically from the ridge on the flanks of volcanoes were interpreted as volcanic and not included in the survey. Box network ridges with low sinuosity and orthogonal junctions were also eliminated. Our criteria differed from the only other planet-wide survey of ridges with high-resolution imagery (Williams, 2007), which cataloged rectilinear ridges independent of local context because sufficient imagery was not available at that time. Features that could help distinguish potential eskers from fluvial ridges require data not available globally (High Resolution Imaging Science Experiment [HiRISE, aboard MRO] or CTX stereo topography), and so were not compatible with a systematic approach; potential eskers were included in our mapping as a separate class. Our criteria are

conservative such that ridges were not included in our survey unless there existed confidence that they represent the vestigial site of a river or subglacial channel on Mars, thus the results reflect a minimum for fluvial depositional areas on Mars. Moreover, as on Earth, most depositional areas are not marked by ridges.

## RESULTS AND DISCUSSION

Our results revealed 68 regions with networks of large ( $> 70$  m width) fluvial ridges—referred to as ridge systems—distributed across Mars with stream orders that ranged from 1 to 4. Eighteen (18) of these systems had not been documented before (Table S1). The 68 systems consist of 539 individual ridges. We captured 94% of previously known ridge systems that match our criteria, providing an estimate of the error resulting from our approach using the massive CTX mosaic (Table S1).

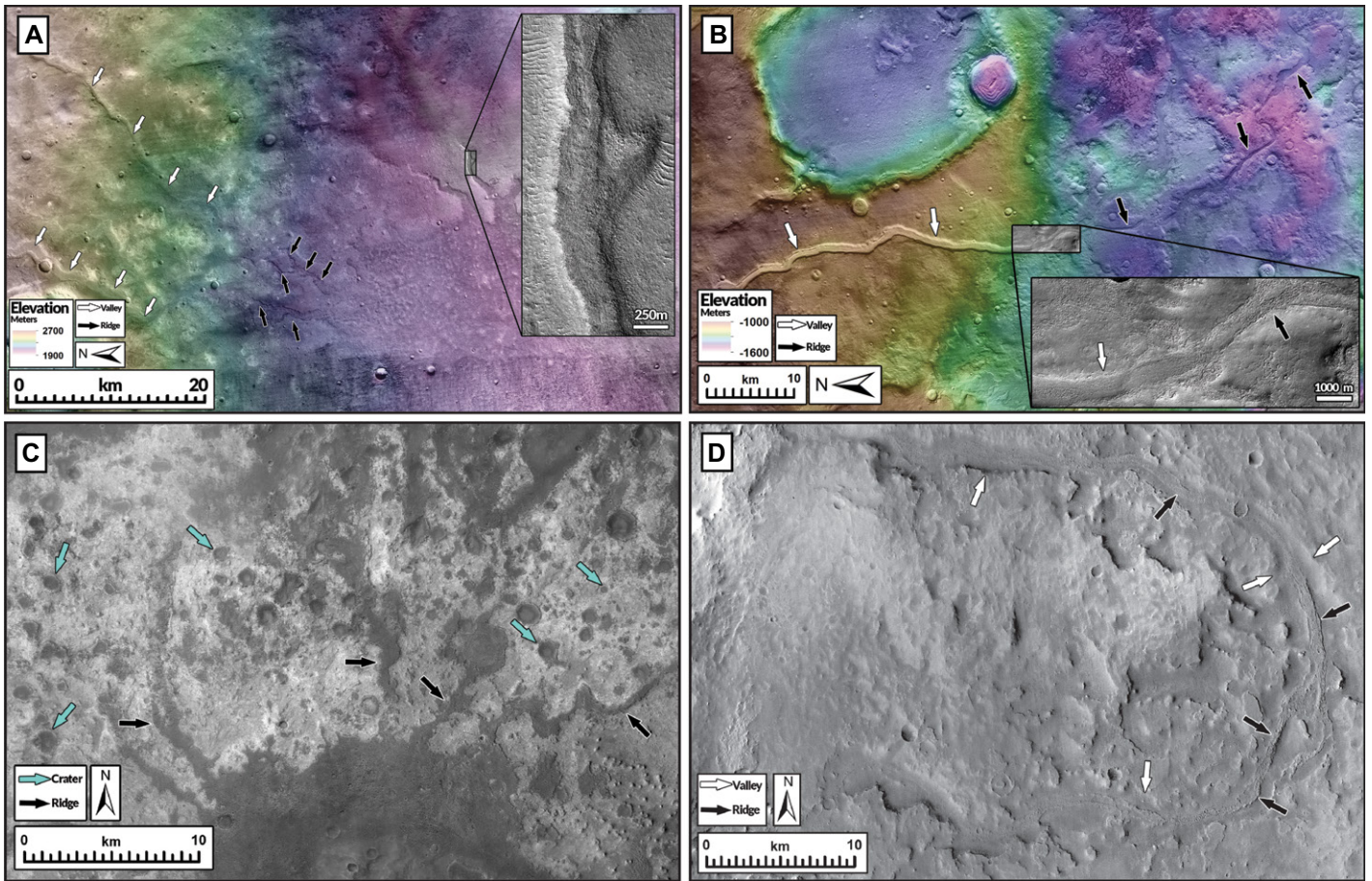


**Figure 2.** (A) NASA Context Camera (CTX) mosaic with Mars Orbiter Laser Altimeter (MOLA) topography of intercrater plains northwest of Argyre and southeast of Thaumasia ( $43.1^{\circ}\text{S}$ ,  $292.4^{\circ}\text{E}$ ). Sinuous ridges compose margins of a low-albedo unit, down gradient from valley networks trending from Thaumasia. Inset: High Resolution Imaging Science Experiment (HiRISE) orbit ESP\_050997\_1365. (B) CTX mosaic with MOLA topography of an unnamed valley network transitioning into a fluvial ridge.  $32.3^{\circ}\text{N}$ ,  $46.0^{\circ}\text{E}$ . Inset: HiRISE orbit PSP\_005355\_2125. (C) CTX mosaic of fluvial ridges in northern Meridiani showing nearby inverted craters not presently in contact with ridges.  $19.9^{\circ}\text{N}$ ,  $343.0^{\circ}\text{E}$ . (D) CTX mosaic of a fluvial ridge preserved within a valley.  $5.46^{\circ}\text{N}$ ,  $352.63^{\circ}\text{E}$ .

Fluvial ridges appear flat-crested at CTX scale with the exception of large networks previously interpreted as eskers (Head and Pratt, 2001; Banks et al., 2009) (blue in Fig. 3A) found at latitudes  $60^{\circ}\text{S}$ – $85^{\circ}\text{S}$ . Our results confirmed that Arabia Terra and the Medusae Fossae Formation host the densest concentrations of fluvial ridges on the planet. This fact yielded a bimodal elevation distribution (Fig. 4B), but fluvial ridges in aggregate are distributed across the southern highlands. Branching (Fig. 1B) and anastomosing (Fig. 1D) ridges are common. Ridges are typically  $<20$  km in length (Fig. 4A), though some extend to 100 km, with the longest being ridges in the Dorsa Argentea Formation. Ridges imaged by HiRISE (Figs. 1A, 2A, and 2B) exhibit a range of textures and patterns that reflect eolian reworking, suggesting that the ridges are an incomplete record of the length of ancient fluvial systems.

Fluvial ridges are most common in the lower extents of the southern highlands (Fig. 3). The Argyre region has ridges downslope from the Thaumasia-Warrego valley networks. Fluvial

ridges were observed in the Hellas region, though they occur sparsely. Two fluvial ridge systems were found within the Isidis region, including deposits observed within the Jezero crater watershed (Fig. 1E).

Ridges were not observed in geologically young terrains, and instead are found within Late Noachian or Early Hesperian units (Figs. 3B and 4C) (Tanaka et al., 2014). The two exceptions are those contained within the Medusae Fossae Formation—the age of these is challenging to ascertain and, based on stratigraphic relationships, could be considerably older than ages reflected in the formation's retained crater population (Kerber and Head, 2010)—and the ridges of the Dorsa Argentea Formation (Head and Pratt, 2001). The Dorsa Argentea Formation unit was mapped as Early Hesperian age (Tanaka et al., 2014), while the superposed crater population of the ridges themselves is consistent with a Late Noachian–Early Hesperian age (Kress and Head, 2015). While direct dating of specific ridge systems is not possible due to their low surface area and history of

modification, which could include small-scale local reactivation, the terrain age estimates coincide with buffered crater-count measurements of cessation ages for valley networks (Fassett and Head, 2008a). Thus, the ridges and valley networks could be coeval.

Fluvial ridges are geographically associated with valley networks. Ridges, on average, occurred at lower elevations (mean =  $-341.5$  m,  $\sigma = 1672.04$  m) than valley networks (Hynek et al., 2010) (mean =  $1177.27$  m,  $\sigma = 2044.85$  m) (Figs. 3A and 4B); a pattern expected in source-to-sink sediment transport systems (Allen, 1997). They also occur, on average, at lower elevations than open-basin lakes (Fassett and Head, 2008b) (mean =  $32.62$  m,  $\sigma = 1519.17$  m) and at comparable elevations to closed-basin lakes (Goudge et al., 2015) (mean =  $-92.78$  m,  $\sigma = 1709.88$  m). All fluvial ridges were observed within terrain that has valley networks upslope, except in the Dorsa Argentea Formation. In specific terrains (Figs. 1A, 2A, and 2B), ridges typically transition from valley networks, and ridges were also found

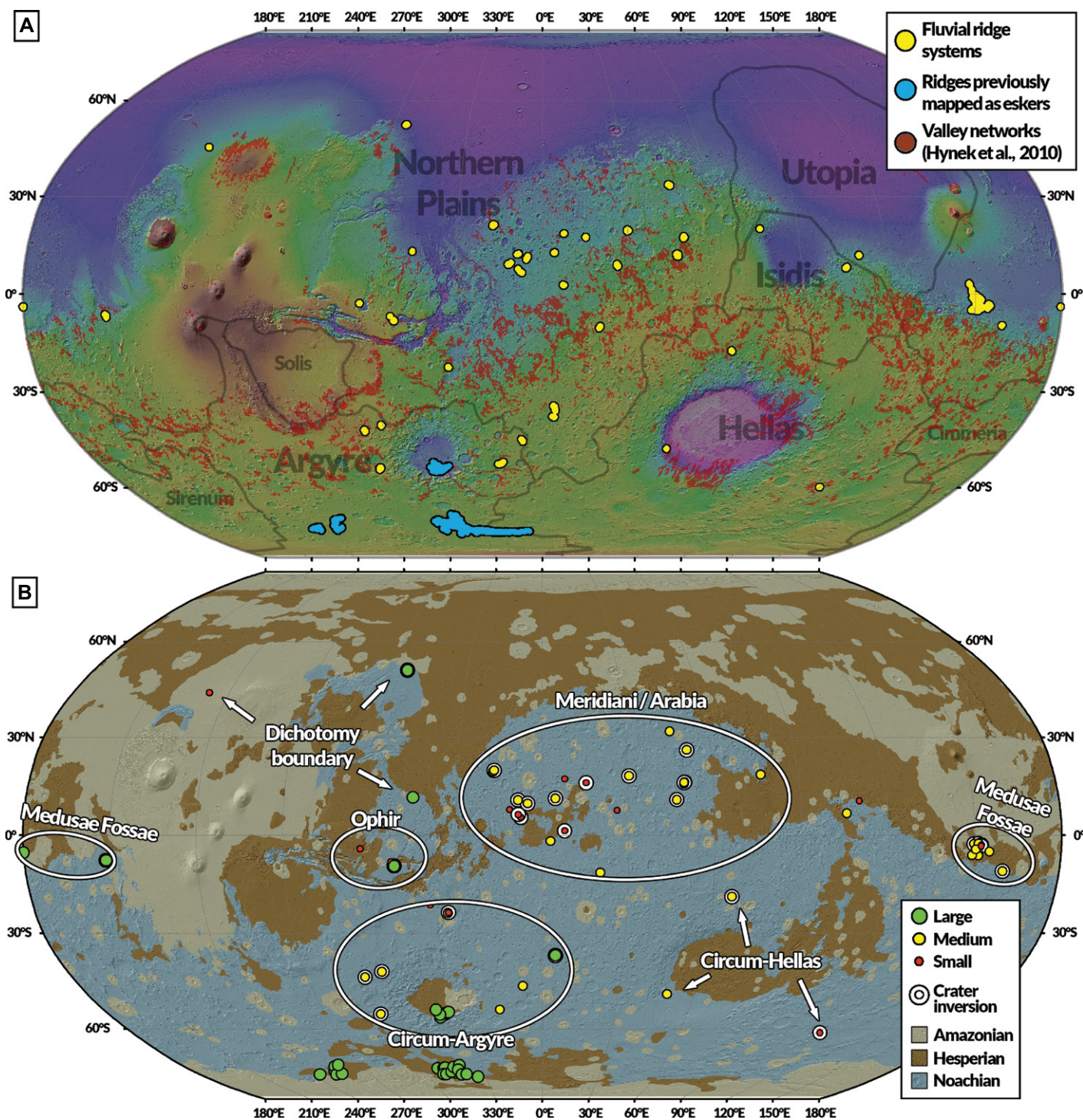


**Figure 3. (A)** Global distribution of systems of fluvial ridges on Mars. Each marker represents a region with many ridges. Eighteen (18) of 68 ridge systems have not been previously mapped (see Table S1 [see footnote 1]). Features previously interpreted as eskers (Head and Pratt, 2001; Banks et al., 2009) have been mapped in blue. Mapped valley networks (Hynek et al., 2010) are shown in red. Major physiographic provinces on Mars are from NASA Mars Orbiter Laser Altimeter data (Banerdt and Vidal, 2001). **(B)** Size of each fluvial ridge system on a simplified age map; from Tanaka et al. (2014). Crater inversion sites contain exhumed crater fills not in contact with fluvial ridges.

within valleys (Figs. 1E and 2D). Our findings are consistent with regional data from Arabia Terra (Davis et al., 2016, 2019) (Fig. 3B). The broader Argyre region has similar relationships, with fluvial ridges down-dip from dense valley-network fields. Ridges were not observed in regions predicted to have been ice fields in

Noachian time (Wordsworth, 2016) or in close proximity to valley networks proposed to be subglacial (Grau Galofre et al., 2020).

Most of the fluvial ridges are found in dense networks and are commonly in contact with broader flat sedimentary strata undergoing erosion (Figs. 1A, 2A, and 2B), sug-

gesting they may have been exhumed from a larger depositional area. Furthermore, fluvial ridges were commonly (43%) found in proximity to inverted craters (Figs. 2C and 3B), further suggesting exhumation of a thick stratigraphic section. In some cases, the ridges and inverted craters are not connected. One

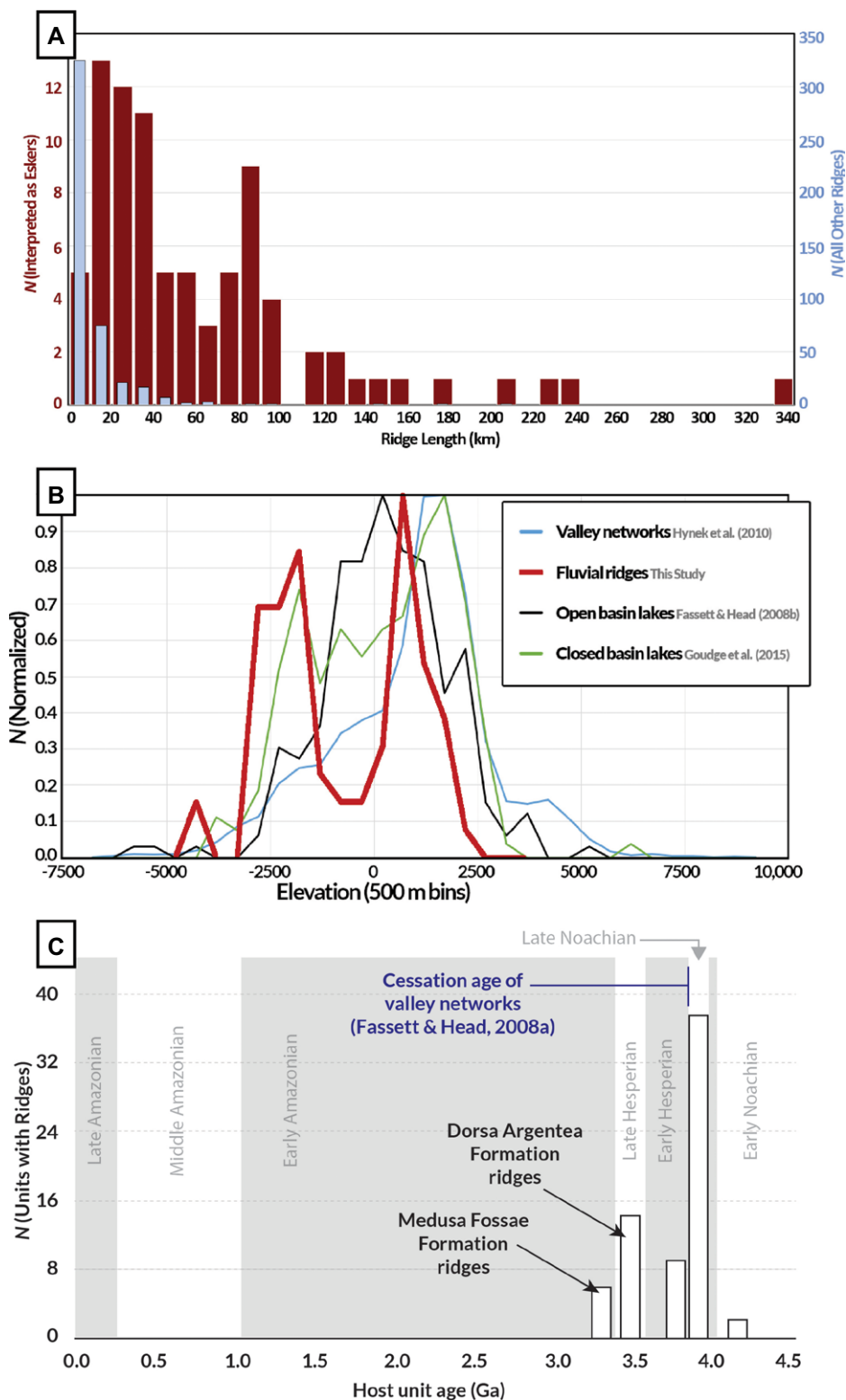


**Figure 4. (A) Histogram of lengths of primary fluvial ridges from all 68 mapped Mars ridge systems (Fig. 3). Ridges that have been interpreted as eskers are plotted in red. (B) Normalized (to the maximum bin) histograms versus elevation using NASA Mars Orbiter Laser Altimeter data from valley networks (Hynek et al., 2010), fluvial ridges, open-basin lakes (Fassett and Head, 2008b), and closed-basin lakes (Goudge et al., 2015). (C) Histograms of fluvial deposition estimated from the ridge host unit (Tanaka et al., 2014).**

explanation for isolated inverted craters is that the sediment filling the crater was sourced by a more regional process (e.g., airfall of ash or

mineralized groundwater deposits) rather than transported by rivers to the crater (Hynek and Phillips, 2001). Another possibility is that the

craters were filled with river-transported sediments (Davis et al., 2019), but that the crater-adjointing river either was not depositional or did not have erosion-resistant deposits necessary to form a ridge, or that the ridge was not preserved during exhumation.

## CONCLUSIONS

The majority of Martian fluvial ridge systems we mapped (61/68, ~90%) occur within poorly constrained topographic boundaries within intercrater plains in the southern highlands. The dominance of large ridges in intercrater plains suggests the possibility of fluvial-influenced depositional areas, tens to hundreds of square kilometers in scale, that are distinct from the smaller alluvial and deltaic fan deposits in craters that have been the focus in previous work (Fassett and Head, 2008b; Kraal et al., 2008; Goudge et al., 2015). These large depositional areas might be akin to sedimentary basins on Earth, but, owing to the thicker Martian lithosphere, they likely lacked the typical tectonic controls seen in terrestrial basins. Future study with higher-resolution data will help delineate the boundaries and character of these broad depositional areas within the highlands.

Our results expand the distribution of ancient fluvial activity to lower elevations from that recognized by the distribution of valley networks, and indicate widespread fluvial deposits that were not crater bound. Moreover, associations in age, geographic location, and elevation indicate that fluvial ridges might represent the downstream depositional equivalent of erosional valley networks. Thus, our systematic mapping results are consistent with the hypothesis (Grotzinger et al., 2013) that, like Earth, Mars may have had distinct regions with net erosional and net depositional river systems, which were linked as source-to-sink sediment transport systems. These depositional areas could contain a rich archive of early Mars climate.

## ACKNOWLEDGMENTS

We thank three anonymous reviewers and the editor for thorough and helpful reviews of this work. We appreciate support from NASA grant NNX16G for this research, and graduate fellowship 80NSSC17K0492 to Hayden.

## REFERENCES CITED

- Allen, P.A., 1997, *Earth Surface Processes*: Hoboken, New Jersey, John Wiley & Sons, 416 p.
- Balme, M.R., Gupta, S., Davis, J.M., Fawdon, P., Grindrod, P.M., Bridges, J.C., Sefton-Nash, E., and Williams, R.M.E., 2020, Aram Dorsum: An extensive mid-Noachian age fluvial depositional system in Arabia Terra, Mars: *Journal of Geophysical Research: Planets*, v. 125, e2019JE006244, <https://doi.org/10.1029/2019JE006244>.
- Banerdt, W.B., and Vidal, A., 2001, Surface drainage on Mars: 32<sup>nd</sup> Lunar and Planetary Science Conference, 12–16 March 2001, Houston, Texas, Abstract 1488.

- Banks, M.E., Lang, N.P., Kargel, J.S., McEwen, A.S., Baker, V.R., Grant, J.A., Pelletier, J.D., and Strom, R.G., 2009, An analysis of sinuous ridges in the southern Argyre Planitia, Mars using HiRISE and CTX images and MOLA data: *Journal of Geophysical Research*, v. 114, E09003, <https://doi.org/10.1029/2008JE003244>.
- Burr, D.M., Enga, M.-T., Williams, R.M.E., Zimbelman, J.R., Howard, A.D., and Brennand, T.A., 2009, Pervasive aqueous paleoflow features in the Aeolis/Zephyria Plana region, Mars: *Icarus*, v. 200, p. 52–76, <https://doi.org/10.1016/j.icarus.2008.10.014>.
- Burr, D.M., Williams, R.M.E., Wendell, K.D., Chojnacki, M., and Emery, J.P., 2010, Inverted fluvial features in the Aeolis/Zephyria Plana region, Mars: Formation mechanism and initial paleodischarge estimates: *Journal of Geophysical Research*, v. 115, E07011, <https://doi.org/10.1029/2009JE003496>.
- Cabrol, N.A., and Grin, E.A., 1999, Distribution, classification, and ages of Martian impact crater lakes: *Icarus*, v. 142, p. 160–172, <https://doi.org/10.1006/icar.1999.6191>.
- Cardenas, B.T., Mohrig, D., and Goudge, T.A., 2018, Fluvial stratigraphy of valley fills at Aeolis Dorsa, Mars: Evidence for base-level fluctuations controlled by a downstream water body: *Geological Society of America Bulletin*, v. 130, p. 484–498, <https://doi.org/10.1130/B31567.1>.
- Carr, M.H., 1996, *Water on Mars*: Oxford, UK, Oxford University Press, 248 p.
- Davis, J.M., Balme, M., Grindrod, P.M., Williams, R.M.E., and Gupta, S., 2016, Extensive Noachian fluvial systems in Arabia Terra: Implications for early Martian climate: *Geology*, v. 44, p. 847–850, <https://doi.org/10.1130/G38247.1>.
- Davis, J.M., Gupta, S., Balme, M., Grindrod, P.M., Fawdon, P., Dickeson, Z.L., and Williams, R.M.E., 2019, A diverse array of fluvial depositional systems in Arabia Terra: Evidence for mid-Noachian to Early Hesperian rivers on Mars: *Journal of Geophysical Research: Planets*, v. 124, p. 1913–1934, <https://doi.org/10.1029/2019JE005976>.
- DiBiase, R.A., Limaye, A.B., Scheingross, J.S., Fischer, W.W., and Lamb, M.P., 2013, Deltaic deposits at Aeolis Dorsa: Sedimentary evidence for a standing body of water on the northern plains of Mars: *Journal of Geophysical Research: Planets*, v. 118, p. 1285–1302, <https://doi.org/10.1002/jgre.20100>.
- Dickson, J.L., Kerber, L.A., Fassett, C.I., and Ehlmann, B.L., 2018, A global, blended CTX mosaic of Mars with vectorized seam mapping: A new mosaicking pipeline using principles of non-destructive image editing, in 49th Lunar and Planetary Science Conference, March 19–23, 2018, The Woodlands, Texas: Lunar and Planetary Institute Contribution 2083, abstract 2480.
- Fassett, C.I., and Head, J.W., III, 2008a, The timing of Martian valley network activity: Constraints from buffered crater counting: *Icarus*, v. 195, p. 61–89, <https://doi.org/10.1016/j.icarus.2007.12.009>.
- Fassett, C.I., and Head, J.W., III, 2008b, Valley network-fed, open-basin lakes on Mars: Distribution and implications for Noachian surface and subsurface hydrology: *Icarus*, v. 198, p. 37–56, <https://doi.org/10.1016/j.icarus.2008.06.016>.
- Goudge, T.A., Aureli, K.L., Head, J.W., Fassett, C.I., and Mustard, J.F., 2015, Classification and analysis of candidate impact crater-hosted closed-basin lakes on Mars: *Icarus*, v. 260, p. 346–367, <https://doi.org/10.1016/j.icarus.2015.07.026>.
- Grau Galofre, A., Jellinek, A.M., and Osinski, G.R., 2020, Valley formation on early Mars by subglacial and fluvial erosion: *Nature Geoscience*, v. 13, p. 663–668, <https://doi.org/10.1038/s41561-020-0618-x>.
- Grotzinger, J.P., Hayes, A.G., Lamb, M.P., and McLennan, S.M., 2013, *Sedimentary processes on Earth, Mars, Titan, and Venus*, in Mackwell, S.J., et al., eds., *Comparative Climatology of Terrestrial Planets*: Tucson, University of Arizona Press, p. 439–472, [https://doi.org/10.2458/azu\\_uapress\\_9780816530595-ch18](https://doi.org/10.2458/azu_uapress_9780816530595-ch18).
- Hayden, A.T., Lamb, M.P., Fischer, W.W., Ewing, R.C., McElroy, B.J., and Williams, R.M.E., 2019, Formation of sinuous ridges by inversion of river-channel belts in Utah, USA, with implications for Mars: *Icarus*, v. 332, p. 92–110, <https://doi.org/10.1016/j.icarus.2019.04.019>.
- Head, J.W., III, and Pratt, S., 2001, Extensive Hesperian-aged south polar ice sheet on Mars: Evidence for massive melting and retreat, and lateral flow and ponding of meltwater: *Journal of Geophysical Research*, v. 106, p. 12,275–12,299, <https://doi.org/10.1029/2000JE001359>.
- Howard, A.D., Moore, J.M., and Irwin, R.P., III, 2005, An intense terminal epoch of widespread fluvial activity on early Mars: 1. Valley network incision and associated deposits: *Journal of Geophysical Research*, v. 110, E12S14, <https://doi.org/10.1029/2005JE002459>.
- Hynek, B.M., and Phillips, R.J., 2001, Evidence for extensive denudation of the Martian highlands: *Geology*, v. 29, p. 407–410, [https://doi.org/10.1130/0091-7613\(2001\)029<0407:EFE DOT>2.0.CO;2](https://doi.org/10.1130/0091-7613(2001)029<0407:EFE DOT>2.0.CO;2).
- Hynek, B.M., Beach, M., and Hoke, M.R.T., 2010, Updated global map of Martian valley networks and implications for climate and hydrologic processes: *Journal of Geophysical Research*, v. 115, E09008, <https://doi.org/10.1029/2009JE003548>.
- Irwin, R.P., III, Howard, A.D., Craddock, R.A., and Moore, J.M., 2005, An intense terminal epoch of widespread fluvial activity on early Mars: 2. Increased runoff and paleolake development: *Journal of Geophysical Research*, v. 110, E12S15, <https://doi.org/10.1029/2005JE002460>.
- Kerber, L., and Head, J.W., 2010, The age of the Medusae Fossae Formation: Evidence of Hesperian emplacement from crater morphology, stratigraphy, and ancient lava contacts: *Icarus*, v. 206, p. 669–684, <https://doi.org/10.1016/j.icarus.2009.10.001>.
- Kraal, E.R., Asphaug, E., Moore, J.M., Howard, A., and Bredt, A., 2008, Catalogue of large alluvial fans in martian impact craters: *Icarus*, v. 194, p. 101–110, <https://doi.org/10.1016/j.icarus.2007.09.028>.
- Kress, A.M., and Head, J.W., 2015, Late Noachian and early Hesperian ridge systems in the south circum-polar Dorsa Argentea Formation, Mars: Evidence for two stages of melting of an extensive late Noachian ice sheet: *Planetary and Space Science*, v. 109, p. 1–20, <https://doi.org/10.1016/j.pss.2014.11.025>.
- Malin, M.C., et al., 2007, Context Camera investigation on board the Mars Reconnaissance Orbiter: *Journal of Geophysical Research*, v. 112, E05S04, <https://doi.org/10.1029/2006JE002808>.
- Miall, A.D., 2010, *Principles of Sedimentary Basin Analysis*: New York, Springer Science & Business Media, 637 p.
- Moore, J.M., and Howard, A.D., 2005, Large alluvial fans on Mars: *Journal of Geophysical Research*, v. 110, E04005, <https://doi.org/10.1029/2004JE002352>.
- Tanaka, K.L., Robbins, S.J., Fortezzo, C.M., Skinner, J.A., and Hare, T.M., 2014, The digital global geologic map of Mars: Chronostratigraphic ages, topographic and crater morphologic characteristics, and updated resurfacing history: *Planetary and Space Science*, v. 95, p. 11–24, <https://doi.org/10.1016/j.pss.2013.03.006>.
- Williams, R.M.E., 2007, Global spatial distribution of raised curvilinear features on Mars, in *Lunar and Planetary Science XXXVIII*, March 12–16, 2007, Houston, TX: Lunar and Planetary Institute Contribution 1338, abstract 1821.
- Williams, R.M.E., Irwin, R.P., III, and Zimbelman, J.R., 2009, Evaluation of paleohydrologic models for terrestrial inverted channels: Implications for application to martian sinuous ridges: *Geomorphology*, v. 107, p. 300–315, <https://doi.org/10.1016/j.geomorph.2008.12.015>.
- Williams, R.M.E., Irwin, R.P., III, Zimbelman, J.R., Chidsey, T.C., and Eby, D.E., 2011, Field guide to exhumed paleochannels near Green River, Utah: Terrestrial analogs for sinuous ridges on Mars, in Garry, W.B., and Bleacher, J.E., eds., *Analogues for Planetary Exploration*: Geological Society of America Special Papers, v. 483, p. 483–505, [https://doi.org/10.1130/2011.2483\(29\)](https://doi.org/10.1130/2011.2483(29)).
- Williams, R.M.E., Irwin, R.P., III, Burr, D.M., Harrison, T., and McClelland, P., 2013, Variability in martian sinuous ridge form: Case study of Aeolis Serpens in the Aeolis Dorsa, Mars, and insight from the Mirackina paleoriver, South Australia: *Icarus*, v. 225, p. 308–324, <https://doi.org/10.1016/j.icarus.2013.03.016>.
- Wordsworth, R.D., 2016, The climate of early Mars: Annual Review of Earth and Planetary Sciences, v. 44, p. 381–408, <https://doi.org/10.1146/annurev-earth-060115-012355>.

Printed in USA